IJCSE International Journal of Computer Sciences and Engineering Open Access
Research Paper Volume-6, Issue-2 E-ISSN: 2347-2693

Reverse Biorthogonal Spline Wavelets in Undecimated Transform for Image Denoising

T.N. Tilak[1*], S. Krishnakumar[2]

[1*]Dept. of Electronics, School of Technology and Applied Sciences, Mahatma Gandhi University, Edappally, India
[2]Dept. of Electronics, School of Technology and Applied Sciences, Mahatma Gandhi University, Edappally, India

[*]*Corresponding Author: tilakd7@gmail.com, Tel.:* +91 9746105280

Available online at: www.ijcseonline.org

Received: 30/Jan//2018, Revised: 09/Feb2018, Accepted: 21/Feb/2018, Published: 28/Feb/2018

***Abstract*—** Reverse biorthogonal wavelets are highly regular wavelets with compact support and symmetric filters and they have explicit construction. This paper explores the performance of the reverse biorthogonal spline wavelets in denoising images differentiated by the detail-contents in the images. The transform used in the study is the Undecimated Wavelet Transform which is a translation-invariant transform. The selected images are corrupted by adding white Gaussian noise to produce noisy test images. The study shows that the denoising effect depends on the amount of details in the image. It is also seen that reverse biorthogonal spline wavelets are highly effective in denoising dense-detail images like fingerprints. These wavelets also give good denoising for low-detail images like human face. The best wavelet in the family for each of these purposes has been sorted out. Rbio 3.1 is found to be an odd member of the family. These wavelets are found to give poor results in denoising medium-detail images. The study finds application in Forensic science and in restoration of facial images and when the images encountered in such applications contain several types of noise distributions simultaneously.

***Keywords*—**Reverse biorthogonal, Spline, Undecimated Transform, Image detail

I. INTRODUCTION

Corrupt images may lead to wrong medical diagnoses, wrong defence decisions, errors in the field of space research and forensic science applications and so on. Therefore image denoising is an important research concern.

Wavelets are little waves generated by means of dilations and translations of a basic function [1]. Image processing using time domain and frequency domain techniques fail to provide time localization of the spectral components of an image, whereas wavelet based processing succeeds in this. This is made possible by the unique feature of wavelets by which they can be dilated (stretched and compressed) and translated. This feature also enables one to observe an image at different scales and hence to investigate the fine as well as coarse details in the image. A "scaling function" which creates the different approximations of the analysed image helps to produce the wavelet basis. There are innumerable wavelets and they belong to different families. The features of wavelets belonging to different families vary widely. It has been commented that "denoising is at the heart of signal representation" [2]. In this paper we investigate the denoising capabilities and shortcomings of the whole family of the 'Reverse Biorthogonal Spline Wavelets' ('Rbio Wavelets').

Rest of the paper is organized as follows: Section II shows the related works, Section III contains the methodology of the study, Section IV describes the results and discussion and Section V concludes the research work.

II. RELATED WORK

Much research has been conducted on wavelet based denoising. To cite a few, it has been determined that bior 1.3 is the most suitable wavelet for denoising medical images [3], symlet wavelet with wiener filter gives good denoising results [4] and reported that "the best choice for medical imaging is not clear" [2] and finding out the best wavelet suitable for any particular application continues to be a challenge for research [5]. Such reports point to the fact that the possibilities in the field of wavelet based denoising have not been explored fully and that there is much to unveil.

III. METHODOLOGY

A. Rbio wavelets

Rbio wavelets are dual spline wavelets which have compact support, biorthogonality and symmetric Finite Impulse Response (FIR) filters. Spline wavelets are highly regular and have explicit construction as opposed to the vast majority of wavelets [6]. The rbio wavelet family comprises a total of 15 wavelets listed as: rbio 1.1, rbio 1.3, rbio 1.5,

rbio 2.2, rbio 2.4, rbio 2.6, rbio 2.8, rbio 3.1, rbio 3.3, rbio 3.5, rbio 3.7, rbio 3.9, rbio 4.4, rbio 5.5 and rbio 6.8.

The inner product of two functions x(t) and y(t) is defined as:

$$< x(t), y(t) > = \int x(t) y^{*}(t) dt \quad (2)$$

where $y^{*}(t)$ is the complex conjugate of y(t). Two bases f_u and g_v together make a set of biorthogonal functions [2],[7] if their inner product satisfies the relation:

$$< f_u, g_v > = \delta(u - v) \quad (3)$$

where $\delta(u - v)$ is the Kronecker delta function described as:

$$\delta(u - v) = \begin{cases} 1, & u = v \\ 0, & u \neq v \end{cases} \quad (4)$$

We always desire symmetric filters because they provide phase linearity, minimize perceptual error and enable better handling of boundaries. We cannot obtain filter symmetry if we employ the analysis filters for synthesis also [8] except in the case of Haar wavelet which has a filter length of two [1]. When we employ biorthogonal wavelets for signal processing the decomposition (analysis) of the signal is carried out with one wavelet and reconstruction (synthesis) is carried out with a different wavelet. This enables one to use symmetric filters of non-trivial lengths and to obtain consequent desirable properties in addition to getting flexibility of design [9]. The matrices of biorthogonal wavelets are invertible and enable perfect reconstruction [2].

B. Algorithm for Wavelet Based Denoising

Investigation of denoising characteristics of a wavelet family essentially consists of the following algorithm:

1. Add noise of desired features to a suitable noiseless test image.
2. Apply the prescribed wavelet transform using the first member of the wavelet family. The wavelet transform then convolves the image with the wavelet filters to decompose it in to 'wavelet coefficients' viz., 'approximation coefficients' and 'detail coefficients'.
3. Apply the prescribed threshold rule to the detail coefficients, to remove noise.
4. Reconstruct the image using the approximation coefficients and the coefficients that survive thresholding, applying the inverse wavelet transform.
5. Estimate the performance metrics values MSE and PSNR.
6. Repeat steps from 2 to 5 with the next member of the wavelet family.
7. Repeat steps from 1 to 6 with the next test image.

C. Test Images

We select three test images for the investigation; these are 'Lena', 'cameraman', and 'fingerprint' which belong to three categories of images viz., low-detail, medium-detail and high-detail types respectively. In this study we assume that the image 'Lena' represents all low-detail images, 'cameraman' represents all medium-detail images and the image 'fingerprint' represents all dense or high-detail images. Each of these images has a size 512x512 pixels.

D. Additive White Gaussian Noise(AWGN)

The noise used for the investigation is '0' mean AWGN with a variance of 0.05 in a 0-1 scale. Gaussian noise is selected for the purpose because it is the most common type of noise found in digital images [10]. The term 'white' implies that the noise has a constant power spectrum [11]. The mean value '0' for the noise simplifies the computations. Being 'additive', the random values of the noise get added to the pixels of the noiseless test images to produce the corrupt images required for the investigation. The Gaussian probability density function (pdf) can approximate an ensemble of different pdfs [12]. Hence this study extends its application to such cases in which the image contains noise of different distributions together.

E. Undecimated Discrete Wavelet Transform(UDWT)

The commonly used Discrete Wavelet Transform (DWT) involves decimation (down-sampling) which makes it not translation-invariant. Hence DWT based denoising may produce artifacts like those arising from Gibbs phenomenon [13]. Therefore we make use of the UDWT which is a translation-invariant transform; it avoids decimation and incorporates upsampling at each stage [14],[15],[16]. We perform three-level decompositions using UDWT for the 'Lena' and 'cameraman' images. It is observed that at decomposition levels exceeding two the reconstructed 'fingerprint' image becomes too blurred to be of any use. Hence only two-level decomposition is made for the 'fingerprint' image.

F. Soft Fixed Form Threshold

We use the Soft Fixed Form threshold rule for denoising; it gives better performance than the other popular threshold rule viz., the hard threshold rule [17]. Soft threshold rule is described by the expression:

$$w_{yt} = \begin{cases} \mathrm{sgn}(w_{xt})(|w_{xt}| - t), & |w_{xt}| \geq t \\ 0, & |w_{xt}| < t \end{cases} \quad (5)$$

where w_{xt} and w_{yt} represent the wavelet coefficients before thresholding and after thresholding respectively and 't' is the value of the threshold [18],[19],[20]. $\mathrm{Sgn}(w_{xt})$ denotes the signum function. The fixed form value of the threshold 't' is the 'universal threshold' given by:

$$t = \sqrt{2\sigma^2 \log(MN)} \quad (6)$$

where σ is the standard deviation, σ^2 the noise variance, and [M,N] the image size [21].

G. Performance Measures

The denoising performance can be measured by calculating the Mean Squared Error (MSE) between the original noiseless image and the denoised image using the formula:

$$\mathrm{MSE} = \frac{1}{\mathrm{m\,n}} \sum_{\mathrm{i}=1}^{\mathrm{m}} \sum_{j=1}^{n} (\mathrm{I(i,j)} - \mathrm{I'(i,j)})^2 \qquad (7)$$

where I and I' are the original image and the reconstructed image respectively; m and n indicate the number of columns and rows in the image. I (i,j) represents the pixel in image I at the i^{th} row and j^{th} column.

The Peak Signal-to-Noise Ratio (PSNR) is another performance metric closely related to the MSE and is given [22],[23] by:

$$\mathrm{PSNR} = 10 \log \left(\frac{255^2}{\mathrm{MSE}} \right) \ \mathrm{dB} \qquad (8)$$

We make use of the MATLAB software for carrying out this study.

IV. Results and Discussion

The original images 'Lena', 'cameraman' and 'fingerprint' are shown in Figures 1(a), 1(c) and 1(e) respectively and the corrupted versions of these images are shown in Figures 1(b), 1(d) and 1(f) respectively. Table 1 shows the MSE and PSNR values of the noisy images.

Figures 2, 3 and 4 show the plots of MSE values of denoised images vs. the rbio wavelets for the images 'Lena', 'cameraman' and 'fingerprint' respectively. In hese figures the X-axes show divisions labelled as 1.1, 1.3,..,.6.8. These values stand for the rbio wavelets 'rbio 1.1', 'rbio 1.3', ...,'rbio 6.8' respectively. The Y-axes show the MSE values obtained on denoising with the different rbio wavelets. It can be seen that in denoising with any particular wavelet in the family the MSE of the denoised image increases as the details in the analysed image increases. As such the MSE values obtained for 'Lena'

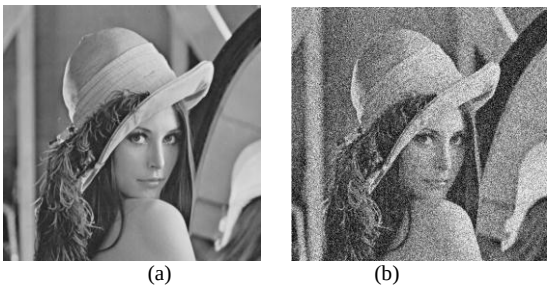

(a) (b)

(c) (d)

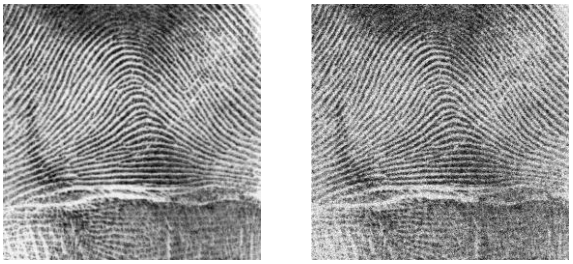

(e) (f)

Figure 1. Original imagesa) 'Lena', (c) 'cameraman', (e) 'fingerprint', and corrupt images (b) 'Lena', (d) 'cameraman' and (f) 'fingerprint'.

have the lowest values and those obtained for 'fingerprint' have the highest values. The MSE values obtained for 'cameraman' fall in between these values. This feature arises from the following fact: 'Lena' being a low-detail image, a large part of the corrupt image contains only noise. Hence a large fraction of the coefficients that result by decomposition of the image have very small amplitudes. Coefficients with small values mostly represent noise in the image and the remaining coefficients correspond to the signal part [24]. These little-valued coefficients which carry most of the noise get removed on thresholding. Hence the denoising is good and the MSE is low. In the case of the dense- detail image 'fingerprint', most of the coefficients that result on decomposition have high values. Hence only a small number of coefficients fall below the threshold and get removed. This implies that only a small part of the noise is eliminated. The additive noise that still remains with the remaining coefficients gives the denoised image a high MSE value. In the case of the medium-detail image 'cameraman', decomposition produces little-valued coefficients and a more or less equal number of high-valued coefficients. Removal of the little-valued coefficients amounts to removal of part of the noise. Hence for denoised 'cameraman' image the MSE values fall in-between the MSE values obtained for 'Lena' and 'fingerprint'. Therefore we reach the conclusion that values of MSE for denoised images are related to the detail contents of the original images. For denoised images the MSE values of low-detail images are low while those of high-detail images are high and the MSE values of medium-detail images fall in between these two ranges of values.

Table 1. MSE and PSNR values of noisy images

Image	'Lena'	'cameraman'	'fingerprint'
MSE	36.49	36.33	109.10
PSNR dB	32.51	32.53	27.75

Now we will look in to the variation in denoising performance with variation in the rbio wavelet used in the

wavelet transform. From Figures 2, 3, and 4 we can observe the following:

1. For all the three images rbio 3.1 gives an abrupt shoot up in MSE value. Figures 5(a) and 5(b) show the scaling function and wavelet function respectively, of the synthesis wavelet of rbio 3.1. As seen in these figures both these functions lack smoothness. The odd behaviour of rbio 3.1 by which it gives a shot up MSE is a consequence of the lack of smoothness of its synthesis functions. Due to this odd nature we skip this wavelet in the discussions that follow.
2. With the other wavelets the MSE values have a zigzag variation as we go from rbio 1.1 through rbio 6.8 in the case of all the three images.
3. The overall lowest MSE and hence the best denoising performance of the rbio family is given by rbio 1.1.
4. For 'Lena', the lowest MSE value is obtained on denoising with rbio 1.1. This lowest MSE value is 11.82 and the corresponding PSNR is 37.40 dB. The increase in PSNR obtained here is 4.89 dB. The smallest increase in PSNR obtained in the family is 4.15 dB. This shows that all the members in the rbio wavelet family give appreciable denoising for the image.
5. For 'fingerprint', the lowest MSE value 34.74 obtained on denoising with level-2 UDWT is got with the same wavelet rbio 1.1. The corresponding PSNR is 32.72 dB and represents an increase by 4.97 dB from the PSNR of the input image. The smallest increase in PSNR obtained in the family is 4.21 dB. This indicates that all the members in the rbio wavelets give good denoising for 'fingerprint'.
6. But denoising the medium detail image 'cameraman' gives lowest MSE 27.44 when rbio 6.8 is used. This

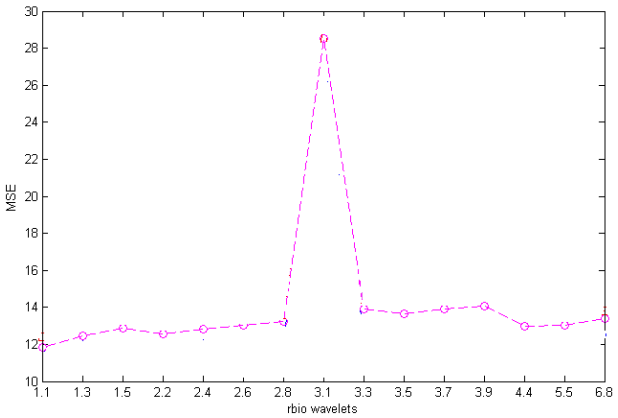

Figure 2. MSE vs rbio wavelets for denoised 'Lena' image

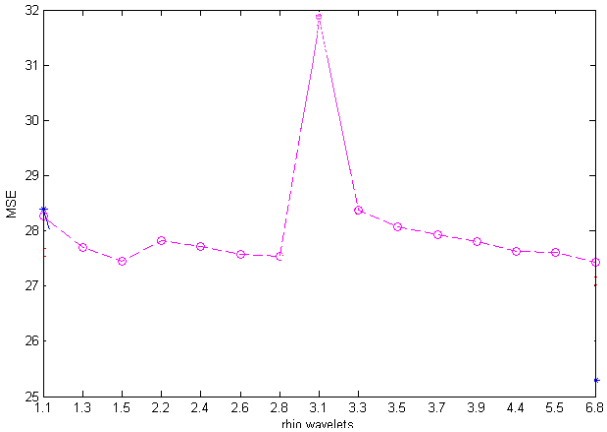

Figure 3. MSE vs rbio wavelets for denoised 'cameraman' image

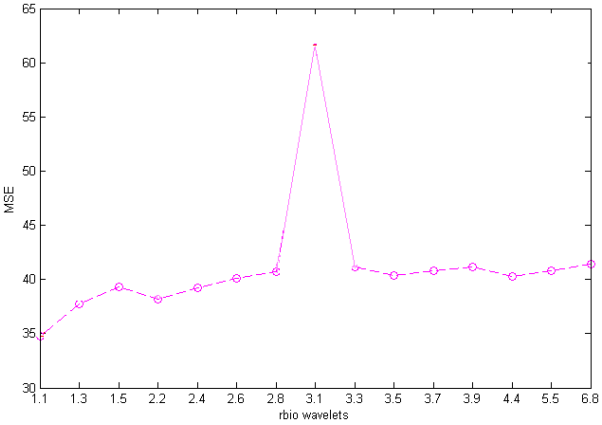

Figure 4. MSE vs. rbio wavelets for denoised 'fingerprint' image

MSE value corresponds to a PSNR of 33.75 dB and a low gain of 1.22 dB in PSNR.

This wide difference in the denoising behaviours of the wavelets can be reasoned as detailed below:

Table 2. Effective lengths of high pass and low pass decomposition filters of rbio wavelets

Wavelet	Effective length of HD	Effective length of LD
rbio 1.1	2	2
rbio 1.3	6	2
rbio 1.5	10	2
rbio 2.2	5	3
rbio 2.4	9	3
rbio 2.6	13	3
rbio 2.8	17	3
rbio 3.1	4	4
rbio 3.3	8	4
rbio 3.5	12	4
rbio 3.7	16	4
rbio 3.9	20	4
rbio 4.4	9	7

rbio 5.5	9	11
rbio 6.8	17	11

First, we consider denoising of the low-detail image 'Lena'. As mentioned earlier a large number of pixels of the corrupt 'Lena' image contain noise only. Table 2 shows the effective lengths, or equivalently the number of non- zero filter taps of the high pass decomposition (HD) filters and the low pass decomposition (LD) filters of the various rbio wavelets. When the wavelet used has a good number of non-zero taps for its HD filter the decomposition of the image results in a large number of coefficients at the high pass filter output. A good part of these coefficients have very small values since a large number of pixels of the corrupt image contains noise only. We apply threshold only to the high pass filtered components [17]. Application of threshold rule to these coefficients removes the small coefficients whose values fall below the threshold. Thresholding operation always results in removal of a part of the signal also [2]. Since the number of coefficients in the high pass filter output is large the amount of signal removed is considerable. Reconstructed image therefore has more error as what can be seen from the high MSE values obtained with rbio wavelets having large HD filter lengths. On the other hand the wavelet rbio 1.1 has the lowest number of filter taps which is two, for its HD filter. Hence convolution of the image with its filters results in only a lesser number of coefficients than those produced in the case of wavelets with more HD filter taps. Consequently application of threshold takes away only a little part of the signal. Hence the reconstructed image has the lowest MSE. Now consider denoising of the dense-detail image. This image has high values for majority of its pixels since the detail-content is high. When the image is decomposed using a wavelet with a large number of HD filter taps the process produces a large number of high pass filtered coefficients just as in the case of low-detail image. But here most of these coefficients have high values unlike with low-detail image. When thresholding operation is applied to these coefficients it is accompanied by attenuation of a part of the signal, as usual. Now the signal attenuation is large, larger than the signal attenuation in the case of low-detail image because now there is larger number of coefficients with high values. This results in a higher MSE value for the reconstructed image. But when we use rbio 1.1 it has only two taps each for its HD and LD filters. Since the number of taps for the HD filter is low the decomposition results in only a small number of high pass coefficients. The thresholding operation affects only this small number of coefficients. The associated signal attenuation is therefore small when compared with the signal attenuation induced by rbio wavelets having longer effective lengths for HD filters. Consequently the MSE value of the denoised image is lowest with rbio 1.1 for high-detail image also.

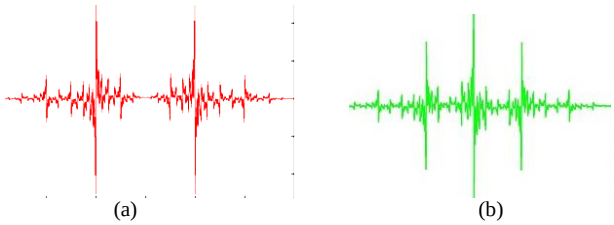

Figure 5. Synthesis functions of rbio 3.1 (a) Scaling function and (b) wavelet function.

Now let us take the case of medium-detail image. This image has large number of pixels with little values or noise only and a more or less similar number of high value pixels. Convolution with the HD filters of rbio wavelets results in a number of high pass filtered coefficients. When the number of HD filter taps is large the number of these high pass coefficients is also large. Since the image is of medium detail the high pass coefficients having high values is more or less equal in number to the high pass coefficients having small values. Removal of the little coefficients by thresholding results in removal of a good part of the noise thus lowering the MSE. But the associated signal attenuation which affects the high pass coefficients having high values keeps the MSE from lowering to the MSE values of low-detail image. When the number of HD filter taps is small, the number of high pass coefficients is small. Being medium-detail image the number of high pass coefficients with low values is still smaller. Hence there is no significant reduction in MSE on their removal by threshold application. Also any increase in MSE due to signal attenuation accompanying thresholding only adds to this.

The number of taps for LD filter is not without any effect in denoising. Instead, it has a significant role in the denoising of the medium-detail image 'cameraman'. From figure 3 we can see that the wavelet rbio 6.8 gives the lowest MSE value for 'cameraman'. For both the other images viz., 'Lena' and 'fingerprint' rbio 1.1 gave the the lowest MSE values. The reason for this difference becomes clear from what follows. From table 2 we can see that the number of taps of the LD filters increases at a high rate for wavelets rbio 3.9 through rbio 5.5. This implies that these wavelets introduce more low pass filtering. The low pass filtered components hold the major part of the signal. Low pass filtering removes most of the noise or high frequency components in the signal to which it is applied. Convolution of the medium detail image 'cameraman' with the low pass filter having large number of taps contributes to a good number of coefficients devoid of noise since the number of LD taps is high. This reduces the MSE of the denoised image. In the case of rbio 6.8 there are 17 HD filter taps and 11 LD filter taps as shown in table 2. The large number of HD filter taps produce a large number of high frequency coefficients a good part of which are of low values because the image is of medium detail. Most of

these low value coefficients fall below threshold value and get removed. This results in a low MSE for the denoised image. The large number of LD filter taps introduces large low pass filtering causing high reduction in MSE. Hence rbio 6.8 gives the denoised image with lowest MSE for the medium-detail image 'cameraman'.

(a) (b)

Figure 6. Denoised images with lowest MSE values (a) 'Lena' and (b) 'fingerprint'

The high rate of increase in the number of LD filter taps for wavelets from rbio 3.9 onwards does not produce a similar result either with the low-detail image 'Lena' or with the high-detail image 'fingerprint'. 'Lena' image on convolution with the LD filter taps produces only a far lesser number of low pass filtered coefficients (devoid of noise) because the image is of low-detail type and greater part of the image is comprised of high-frequency or noise components only. Hence the reduction in MSE due to the jump in number of LD filter taps is not noticeable. The 'fingerprint' image, on the other hand, is dense in detail content. The majority of pixels have high values. Signal attenuation accompanying application of threshold affects this vast majority of pixels. This results in high MSE values. This effect outweighs any decrease in MSE due to increase in number of LD taps.

The results show that rbio wavelets are very good for denoising high-detail images and also low-detail images. The highest percentage reductions in MSE for the three images are: 67.60%, 68.16% and 24.46% respectively for Lena, Fingerprint and cameraman. Rbio 1.1 gives the best denoising performance for both low-detail and high-detail images. Especially rbio 1.1 gives drastic noise reduction performance when applied to a fingerprint image as verified by the large reduction in MSE. This has far-reaching significance especially in forensic science. Also the promising result obtained with rbio 1.1 in denoising the low-detail image 'Lena' shows that this wavelet can be applied for denoising corrupt facial images. Since we get only approximately a low 24.5% maximum reduction in MSE on denoising 'cameraman' image we can conclude that the denoising performance is poor for medium-detail images. Figures 6(a), and 6(b) show the denoised images 'Lena' and 'fingerprint' with lowest MSE values, respectively. These images are found to be good since they preserve the edges in the respective original images and do not exhibit artifacts. Figure 7 shows rbio 1.1 which is the rbio wavelet that has given the best denoising performance for the low-detail image 'Lena' and the high-detail image 'fingerprint'. In this figure the left part (a) shows the analysis wavelet and the right part (b) shows the synthesis wavelet of the dual wavelet. For this particular wavelet pair the synthesis and analysis wavelets coincide.

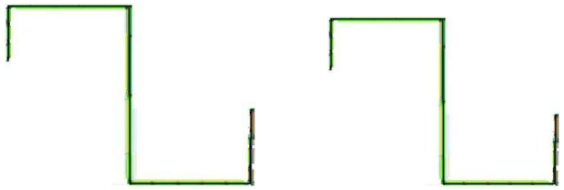

Figure 7. rbio 1,1 (a) analysis wavelet and (b) synthesis wavelet

V. CONCLUSION

On denoising images using reverse biorthogonal spline wavelets the MSE values of denoised images are found to depend directly on the amount of details in the image. The denoising performance metric takes a zigzag variation as the wavelet selected for denoising any particular image is changed from the first member through the last member of the rbio wavelet family, i.e., rbio 1.1 through rbio 6.8. All members in the family, except rbio 3.1, give good performance in denoising low-detail images like face of humans. Rbio 1.1 gives the best denoising for such images, an MSE as low as 11.82 and a corresponding high PSNR of 37.40 dB denoting an increase in PSNR by 4.89 dB could be obtained with this wavelet.. This is a promising result applicable for restoring noisy facial images. The rbio wavelets are also effective in denoising dense-detail images. Rbio 1.1 gives the best denoising performance in the wavelet family for denoising of dense-detail images. A reduction in MSE by 68.16% denoting an increase in PSNR by 4.97 dB could be obtained for fingerprint image when denoised using rbio 1.1. This highly promising result shows that the wavelet rbio 1.1 has potential scope for application in the field of Forensic science. It is also found that the rbio family of wavelets gives only poor results in denoising medium-detail images. The wavelet rbio 3.1 in this family is found to be very poor for denoising application. The results of this study can also be applied when the noise in an image is the joint effect of several types of noise distributions.

REFERENCES

[1] I. Daubechies, *"Orthonormal Bases of Ccompactly Supported Wavelets"*, Communications on Pure and Applied Mathematics. XLI, pp. 909-996, 1988

[2] G. Strang, T. Nguyen, *"Wavelets and filter banks"*, Wellesley-Cambridge Press, Wellesley, pp.xi-71,1996.

[3] Y.S. Bahendwar, G.R. Sinha, *"Mathematical Methods and Systems in Science and Engineering",* WSEAS Press, Spain, pp.158 – 162, 2015.

[4] J. Kaur, R. Kaur, *"Biomedical Images Denoising Using Symlet Wavelet with Wiener Filter"*. International Journal of Engineering Research and Applications (IJERA), Vol. 3, No. 3, pp. 548-550, 2013

[5] L. Renjini, R.L. Jyothi, *"Wavelet Based Image Analysis: a Comprehensive Survey",* International Journal of Computer Trends and Technology (IJCTT), Vol. 21, No.3, pp.134-140, 2015

[6] M. Unser, *"Ten Good Reasons for Using Spline Wavelets."* Proceedings of SPIE, Wavelets Applications in Signal and Image Processing V, 3169, pp. 422-431, 1997.

[7] P.P. Vaidyanathan, I. Djokovic, *"An Introduction to Wavelet Transforms",* California Institute of Technology, Pasadena, pp. 1-116, 1994.

[8] A. Cohen, I. Daubechies, J.C. Feauveau, *"Biorthogonal Bases of Compactly Supported Wavelets"*, Communications on Puree and Applied Mathematics, XLV, pp. 485-560, 1992

[9] M. Vetterli, C. Herley, *"Wavelets and Filter Banks: Ttheory and Design",* IEEE Transactions on Signal Processing, Vol. 40, No. 9, pp. 2207-2232, 1992.

[10] L. Passrija, A.S. Virk, M. Kaur, *"Performance Evaluation of Image Enhancement Techniques in Spatial and Wavelet Domains",* International Journal of Computers & Technology, Vol.3, No.1, pp. 162-166, 2012.

[11] P. Rakheja, R. Vig, *"Image Denoising Using Combination of Median Filtering and Wavelet Transform",* International Journal of Computer Applications, Vol. 141, No.9, pp. 31-35, 2016

[12] T.N. Tilak, S. Krishnakumar, *"Effectiveness of Symlets in De-noising Fingerprint Images",* International Journal of Computer Science and Engineering, Vol. 3, No.12, pp. 29-34, 2015.

[13] R.R. Coifman, D.L. Donoho, *"Translation-Invariant Denoising",* Stanford University, California, pp. 1-26, 1995.

[14] J.L. Starck, J. Fadili, F. Murtagh, *"The Undecimated Wavelet Decomposition and Its Reconstruction",* IEEE Transactions on Image Processing, Vol.16, No.2, pp. 297-309, 2007.

[15] I.W. Selesnick, *"The Double-Density Dual-Tree DWT",* IEEE Transactions on Signal Processing, Vol. 52, No.5, pp. 1304-1314, 2004.

[16] G.P. Nason, B.W. Silverman, *"Wavelets and statistics",* Springer-Verlag, New York, pp. 281–299, 1995.

[17] S.G. Chang, B. Yu, M. Vetterli, *"Adaptive Wavelet Thresholding for Image Denoising and Compression"*, IEEE Transactions on Image Processing, Vol.9, No.9, pp. 1532-1546, 2000.

[18] W. Qian, *"Research on Image Denoising With an Improved Wavelet Threshold Algorithm",* International Journal of Signal Processing, Image Processing and Pattern Recognition, Vol.8, No.9, pp. 257-266, 2015.

[19] L. Gabralla, H. Mahersia, M. Zaroug, *"Denoising CT Images Using Wavelet Transform",* International Journal of Advanced Computer Science and Applications (IJACSA), Vol.6, No.5, pp.125-129, 2015.

[20] L. Yuan, J. Wu, S. Li, *"Improved Wavelet Threshold for Gray Scale Image Denoising",* International Journal of Signal Processing, Image Processing and Pattern Recognition, Vol.7, No.3, pp. 45-52, 2014.

[21] Anutam, Rajini, *"Comparative Analysis of Filters and Wavelet Based Thresholding Methods for Image Denoising",* Computer Science & Information Technology (CS & IT). pp. 137–148, 2014.

[22] K.V. Thakur, P.G. Ambhore, A.M. Sapkal, "*Medical image denoising using rotated wavelet filter and bilateral filter",* IJAIS Proceedings of 7th International Conference on Communication Computing and Virtualization ICCCV, India, pp. 14-18, 2016.

[23] H. Jagadish, J. Prakash, *"A New Approach for Denoising Remotely Sensed Images Using DWT Based Homomorphic Filtering Techniques",* International Journal of Emerging Trends & Technology in Computer Science (IJETTCS), Vol.3, No.3, pp. 90-96, 2014.

[24] S. Bhatnagar, R.C. Jain, *"Application of Discrete Multi-Wavelet Transform in Denoising of Mammographic Images",* Indian Journal of Science and Technology, Vol.9, No.48, pp. 1-9, 2016.

